Textural Feature Selection for Enhanced Detection of Stationary Humans in Through-the-Wall Radar Imagery

A. Chaddad[a], F. Ahmad[a], M. G. Amin[a], P. Sévigny[b], and D. DiFilippo[b]

[a]Radar Imaging Lab, Center for Advanced Communications, Villanova University, 800 Lancaster Ave, Villanova, PA 19085, USA;
[b]Radar Sensing and Exploitation, Defence R&D Canada, 3701 Carling Ave., Ottawa, ON, Canada K1A 0Z4

ABSTRACT

Feature-based methods have been recently considered in the literature for detection of stationary human targets in through-the-wall radar imagery. Specifically, textural features, such as contrast, correlation, energy, entropy, and homogeneity, have been extracted from gray-level co-occurrence matrices (GLCMs) to aid in discriminating the true targets from multipath ghosts and clutter that closely mimic the target in size and intensity. In this paper, we address the task of feature selection to identify the relevant subset of features in the GLCM domain, while discarding those that are either redundant or confusing, thereby improving the performance of feature-based scheme to distinguish between targets and ghosts/clutter. We apply a Decision Tree algorithm to find the optimal combination of co-occurrence based textural features for the problem at hand. We employ a K-Nearest Neighbor classifier to evaluate the performance of the optimal textural feature based scheme in terms of its target and ghost/clutter discrimination capability and use real-data collected with the vehicle-borne multi-channel through-the-wall radar imaging system by Defence Research and Development Canada. For the specific data analyzed, it is shown that the identified dominant features yield a higher classification accuracy, with lower number of false alarms and missed detections, compared to the full GLCM based feature set.

Keywords: Through-the-wall radar imaging, feature selection, target detection, co-occurrence matrix.

1. INTRODUCTION

Through-the-wall radar imaging (TWRI) covers a broad range of applications in both civilian and military contexts, ranging from surveillance and reconnaissance to hostage rescue missions and searching for survivors in natural disasters. One of the primary objectives of TWRI is to provide means for detection of stationary humans obscured by walls.[1,2] This highly desirable objective is challenged by the presence of strong clutter caused by the electromagnetic (EM) scatterings from the building structure and other stationary indoor objects, and also by the rich multipath returns resulting from target interactions with the indoor environment. The losses encountered by the signal due to the presence of exterior and interior walls between the radar and the targets limit the use of biometric features, such as breathing and heartbeat, for identifying stationary humans inside buildings. As such, despite the presence of clutter and multipath ghosts in radar images, most of the efforts related to stationary indoor target detection have been focused solely on the development of effective techniques in the image domain.[3-7]

Feature-based methods have shown promise in discriminating the true targets from multipath ghosts and clutter that closely mimic the targets in size and intensity in through-the-wall radar imagery.[7,8] More specifically, target and clutter discriminating characteristics in synthetic aperture radar (SAR) based indoor images have been captured through textural feature extraction from the gray level co-occurrence matrices (GLCM). GLCMs encapsulate the local spatial relationships among the gray levels of neighboring image pixels and have found widespread application in optical and medical image analyses.[9-11] Five commonly used co-occurrence based textural features, namely, contrast, correlation, energy, entropy, and homogeneity, are obtained from known target and ghost/clutter regions in through-the-wall radar images and are used to train a minimum distance classifier.[7]

*fauzia.ahmad@villanova.edu; http://www1.villanova.edu/villanova/engineering/research/centers/cac/facilities/rillab.html

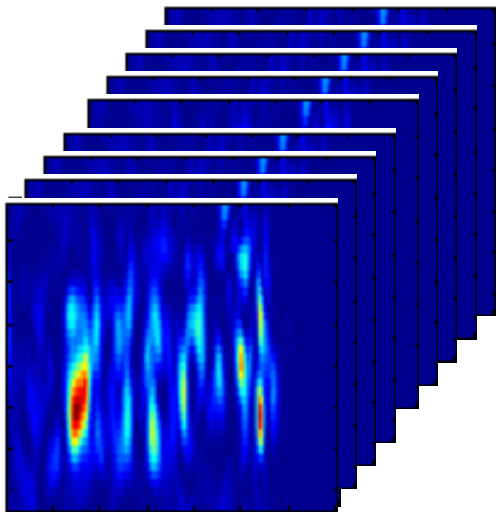

Figure 1. Example of a 3D SAR image, based on real data experiments conducted by DRDC.

In this paper, we address the task of feature selection in order to identify a relevant subset of the aforementioned five co-occurrence features, while discarding those that are either redundant or confusing, thereby improving the performance of the feature based detection technique of Ref. [7]. A Decision Tree algorithm[12] is applied to find the optimal combination of features for the classification problem at hand. A K-Nearest Neighbor (KNN) classifier[13,14] is employed for performance evaluation of the identified dominant features in terms of their target and ghost discrimination capability and comparison with the full feature set. To this end, we use real three-dimensional (3D) images acquired with the vehicle-borne multi-channel through-the-wall radar imaging system developed by Defence Research and Development Canada (DRDC).[15] The specific dataset corresponds to through-the-wall measurements of a small room with six human occupants, with one person sitting on the floor while the others standing at various locations. We show that, for the specific data analyzed, the energy and entropy are identified as the dominant textural features and provide superior classification performance over the full feature set.

The remainder of the paper is organized as follows. Section 2 reviews the co-occurrence featured based detection technique, highlighting the five considered textural features. Feature selection based on decision trees is presented in Section 3. Performance comparison of the identified dominant features and the full feature set using real images is provided in Section 4. Section 5 provides the conclusion.

2. CO-OCCURRENCE FEATURE BASED DETECTION TECHNIQUE

In this section, we review the co-occurrence feature based image domain detection scheme proposed in Ref. [7] for target and clutter/ghost discrimination in TWRI.

Consider a 3D image of size $N \times M \times L$, whose pixels can assume an intensity value from the set $\{0, 1, ..., J-1\}$, where J denotes the total number of intensity levels. Figure 1 shows an example of such a 3D SAR through-the-wall image.

2.1 Gray Level Co-occurrence Matrix

A co-occurrence matrix is defined as a two-dimensional (2D) histogram of gray levels for a pair of pixels, which are separated by a fixed spatial relationship, specified in terms of distance and direction. With J as the total number of intensity levels in the image under consideration, the (p, q)-th element of a $J \times J$ GLCM $\boldsymbol{G}_{\boldsymbol{d}}$, corresponding to displacement $\boldsymbol{d} = (d_x, d_y, d_z)$, is the relative frequency with which two neighboring pixels displaced by $\boldsymbol{d}$ occur in the image, one with gray level p, and the other with gray level q. Formally, the (p, q)-th element of $\boldsymbol{G}_{\boldsymbol{d}}$ reads as[16]

$$\boldsymbol{G}_{\boldsymbol{d}}(p,q) = \sum_{n=1}^{N}\sum_{m=1}^{M}\sum_{l=1}^{L}\begin{cases}1 & \text{if } I(n,m,l) = p \text{ and } I(n+d_x, m+d_y, l+d_z) = q \\ 0 & \text{otherwise}\end{cases} \tag{1}$$

where $p,q = 0,1,\ldots,J-1$, and $I(n,m,l)$ and $I(n+d_x, m+d_y, l+d_z)$ are the intensity values of the two pixels with the spatial relationship $\boldsymbol{d}$. Typically used values for the displacement $\boldsymbol{d}$ comprise an offset of one to two pixels in thirteen possible directions represented by azimuth ϕ and elevation θ, each ranging from 0° to 135° in 45° increments.[16,17]

After constructing the GLCM for a given $\boldsymbol{d}$, we normalize the GLCM so that the sum of its elements is equal to 1. That is, the (p, q)-th element of the normalized GLCM is given by

$$\overline{\boldsymbol{G}}_{\boldsymbol{d}}(p,q) = \frac{\boldsymbol{G}_{\boldsymbol{d}}(p,q)}{\sum_{p=0}^{J-1}\sum_{q=0}^{J-1}\boldsymbol{G}_{\boldsymbol{d}}(p,q)}. \tag{2}$$

Then, $\overline{\boldsymbol{G}}_{\boldsymbol{d}}(p,q)$ is the joint probability of occurrence of pixel pairs with a defined spatial relationship $\boldsymbol{d}$ having gray level values p and q in the 3D image.

2.2 Feature Extraction

Five different features, namely, contrast, correlation, energy, entropy, and homogeneity, are extracted from each normalized GLCM.[7, 9, 17] *Contrast* measures the amount of local intensity variations present in the image and is defined as

$$Contrast = \sum_{p,q}(p-q)^2\overline{\boldsymbol{G}}_{\boldsymbol{d}}(p,q) \tag{3}$$

The c*orrelation* feature is a measure of gray level linear dependencies in the image and is given by

$$Correlation = \sum_{p,q}\frac{(p-\mu_1)(q-\mu_2)\overline{\boldsymbol{G}}_{\boldsymbol{d}}(p,q)}{\sigma_1\sigma_2} \tag{4}$$

where μ_1, σ_1, and μ_2, σ_2 are the means and standard deviations of the respective marginal distributions $\overline{\boldsymbol{G}}_{\boldsymbol{d}}^{1}(p) = \sum_{q}\overline{\boldsymbol{G}}_{\boldsymbol{d}}(p,q)$ and $\overline{\boldsymbol{G}}_{\boldsymbol{d}}^{2}(q) = \sum_{p}\overline{\boldsymbol{G}}_{\boldsymbol{d}}(p,q)$ associated with the normalized GLCM. The *energy* feature measures the textural uniformity and is defined as

$$Energy = \sum_{p,q}(\overline{\boldsymbol{G}}_{\boldsymbol{d}}(p,q))^2 \tag{5}$$

The *entropy* feature measures the disorder or complexity of the image and is defined as

$$Entropy = \sum_{p,q}\overline{\boldsymbol{G}}_{\boldsymbol{d}}(p,q)\log\overline{\boldsymbol{G}}_{\boldsymbol{d}}(p,q) \tag{6}$$

Finally, the *homogeneity* feature measures the closeness of the distribution of elements in the co-occurrence matrix to the co-occurrence matrix diagonal. It is defined as

$$Homogeneity = \sum_{p,q}\frac{1}{1+|p-q|}\overline{\boldsymbol{G}}_{\boldsymbol{d}}(p,q) \tag{7}$$

For the through-the-wall stationary human detection problem, the aforementioned textural features are extracted from the GLCM's for the aforementioned twenty-six displacement vectors. Therefore, the length of the resulting feature vector is 130. It is noted that, instead of the entire image, the textural feature vectors are computed for known target and ghost/clutter regions for the training set and for those regions of the test 3D image, which are identified as candidate target regions.

2.3 K-NN Classifier

We employ a simple supervised learning algorithm, namely, the K Nearest Neighbors classifier, which is commonly used in learning and classification. Therein, an object is classified based on the "distance" of its features from those of its neighbors, with the object being assigned to the class most common among its K nearest neighbors.[14] Euclidean distance is the commonly used distance metric. The neighbors are taken from a set of objects, called the training set, for which the correct classification is known.

- If K = 1, the algorithm simply becomes nearest neighbor algorithm and the object is classified to the class of its nearest neighbor.
- If K >1, the object is assigned to the class of the majority of its K nearest neighbors.

Typically, K is chosen to be odd when the number of classes is 2 to resolve any ties. A higher K increases the classification accuracy but at the expense of computational time.

2.4 Performance Metrics

We consider three metrics, namely, accuracy, missed detection rate, and false alarm rate, to provide a quantitative assessment of the classification technique. These metric are defined as follows.

$$Accuracy = \frac{\text{Number of objects correctly classified}}{\text{Total number of objects}} \tag{8}$$

$$Missed\ \ Detections = \frac{\text{Number of targets incorrectly classified}}{\text{Total number of objects}} \tag{9}$$

$$False\ \ Alarms = \frac{\text{Number of ghosts/clutter incorrectly classified}}{\text{Total number of objects}} \tag{10}$$

3. FEATURE SELECTION

We consider decision tree analysis to identify a subset of the considered features that is most relevant for distinguishing targets from clutter/ghost regions in the 3D images. Decision tree based scheme is a nonparametric approach which does not require any prior assumptions about the probability distributions of the various features.[20] A decision tree is a hierarchical structure, which consists of directed edges and three type of nodes: i) A root node that has no incoming edges and zero or more outgoing edges, ii) Internal nodes, each of which has exactly one incoming edge and two or more outgoing edges, and iii) Leaf or terminal nodes, each of which has exactly one incoming edge and no outgoing edges. The tree is typically grown as a recursive partitioning of the training samples into successively purer subsets. If all of the training samples associated with a particular node t belong to the same class, then t is a leaf node and gets assigned a class label. On the other hand, if the training samples associated with node t belong to different classes, then a single feature test condition is chosen to separate the sample points into smaller subsets. A child node is created for each outcome of the test condition and the records associated with the parent node t are distributed to the children based on the outcomes. The algorithm is then recursively applied to each child node until a stopping criterion is met.

For the target and clutter/multipath discrimination problem, there are only two classes and the considered features take continuous values. As such, the test condition at the root and internal nodes takes the form of a comparison test with binary outcomes. That is, the feature value is compared to a threshold and the training samples are split accordingly. The design issues that need to be addressed are i) the determination of appropriate thresholds for the various features, and ii) the selection of the best feature to use at a particular node for making the split. For the latter, a goodness criterion is used to determine how well the various feature test conditions perform. A typical strategy is to select the feature test condition that minimizes the weighted average Δ of an impurity measure $H(\cdot)$ of the child nodes, given by

$$\Delta = \sum_{i=0}^{1} \frac{Q_i}{Q} H(v_i) \tag{11}$$

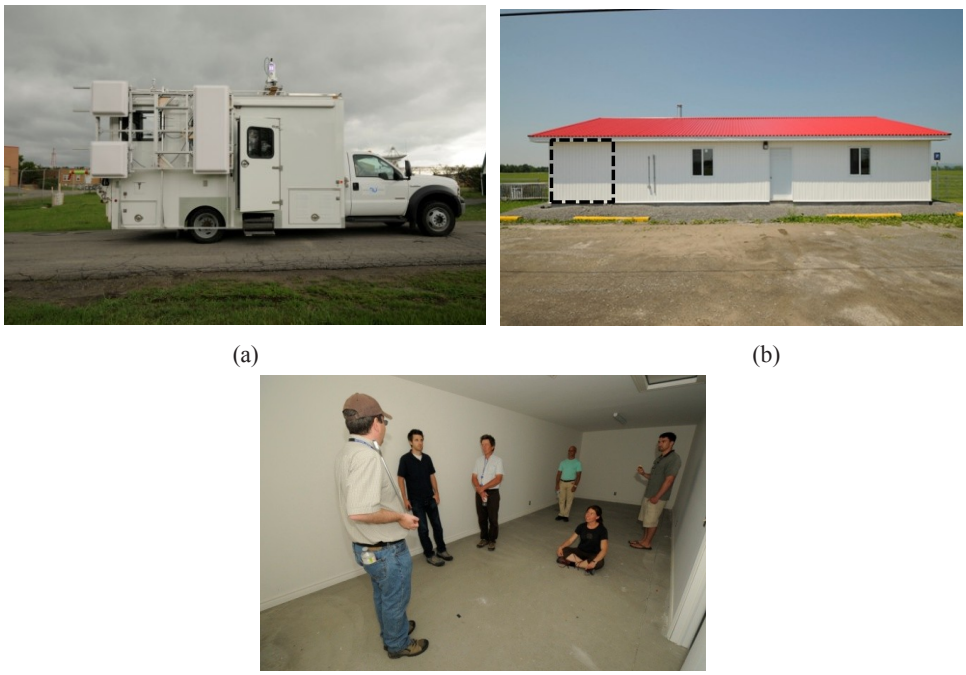

(a) (b)

(c)

Figure 2. (a) Through-the-wall MIMO System. (b) Building used for Through-the-Wall Measurements (the dashed square indicates the room containing the human targets. (c) Scene with six human subjects. Photos by J. Lang, DRDC Ottawa.

where Q is the total number of training samples at the parent node t and Q_i is the number of training samples associated with the child node v_i. The Gini index is a commonly used impurity measure, which is defined for the underlying two-class problem as

$$H_{gini}(v_i) = 1 - \sum_{j=1}^{1} [P(j \mid v_i)]^2, \quad P(1 \mid v_i) = 1 - P(0 \mid v_i) \tag{12}$$

with $P(j \mid v_i)$ being the fraction of samples belonging to class j at a given node v_i.

For each feature 'X', the threshold for the comparison test can also be determined by using the weighted average of the Gini index. The training samples are first sorted based on the values they take for the feature X and candidate thresholds are identified by taking the midpoints between two adjacent sorted values. For each candidate threshold, the data set is scanned to count the number of training samples less than or greater than the candidate. The Gini index values for the corresponding child nodes and their weighted average is then computed. The candidate that produces the lowest weighted average of the Gini index is chosen as the threshold for feature X.

4. EXPERIMENTAL RESULTS

We use real 3D images collected with DRDC's through-the-wall multi-channel radar system.[15] The radar is installed inside a vehicle with its two transmit antennas and an eight-element receive array mounted on the side of the vehicle, as shown in Fig. 2(a). The antenna elements are compact Y-shaped printed bowtie antennas and, when used in the vertical polarization, have approximately 60º beamwidth in the elevation direction and 150º beamwidth in the azimuth or horizontal direction.[18] The receive array has an inter-element spacing of 15 cm, and the two transmit antennas are separated by 1.2 m. The transmit and receive array antennas have a horizontal spacing of 2 m. A frequency-modulated continuous wave signal covering the 0.8 to 2.7 GHz frequency band is used as the transmit signal. A switch is used to alternate the radar transmissions between the two transmit antennas, and the eight-channel radar receiver digitizes the eight received signals for each radar transmission.

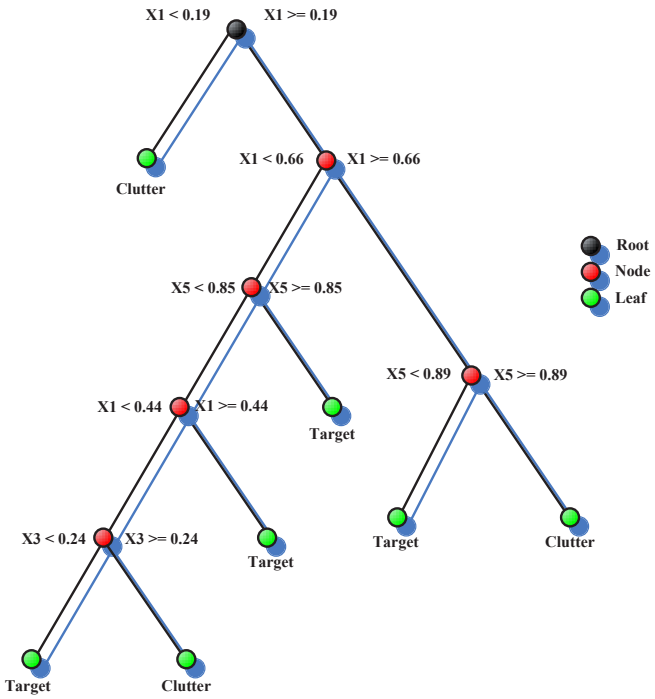

Figure 3. Decision tree grown using 5 attributes extracted from 26 GLCMs using 11 target and 11 clutter regions. The labels X1, X2, X3, X4, and X5 denote energy, contrast, correlation, homogeneity, and entropy, respectively.

A small room in the Troop Shelter building, shown in Fig. 2(b), was imaged three different times, with six, four, and one human occupant, respectively. The antennas were lowered on the van between measurements from the first scene and the latter scenes, which resulted in a considerable increase in clutter. Fig. 2(c) depicts the scene with the six human targets. The exterior walls of the building are constructed of vinyl, chip board and drywall on a 16 in. spacing wood stud frame. The raw radar data were collected while the vehicle moved along a straight path parallel to the front wall of the building, allowing 3D images to be generated in downrange, azimuth, and elevation using backprojection.

Eleven target regions and eleven clutter regions were extracted from the 3D through-the-wall images. GLCM computations corresponding to the 26 displacements were carried out, followed by the extraction of the 130-element textural feature vectors, for each target and clutter regions. Thus, we had a total of 11 target feature vectors and an equal number of clutter feature vectors.

4.1 Decision Tree Analysis

We applied decision tree analysis to determine the dominant extracted features, which would provide reliable discrimination between the targets and clutter. In order to reduce the computational complexity and improve the ease of interpretation, we chose not to identify dominant features from amongst the 130 total features. Rather, we decided to determine the dominant attribute from amongst contrast, correlation, energy, entropy, and homogeneity. Thus, the values taken by these attributes under different displacements served as additional training sample points for the target and clutter classes. Figure 3 shows the resulting decision tree. We observe that energy and entropy play a dominant role as they appear towards the top of the tree structure, whereas correlation comes in a distant third. Homogeneity and contrast have been identified as irrelevant attributes for the classification problem at hand since they do not appear in the tree.

4.2 Classification Performance Comparison

We first performed classification using the full feature set, i.e., the feature vector of length 130. Because of the availability of limited data (only 11 targets and 11 clutter samples), we used leave-one-out cross validation,[19] wherein the classification was performed 22 times, using one feature vector from the dataset for testing and the remaining for

Table 1. Performance comparison between the dominant features and the full feature set.

Performance Metric	Full Feature Set	Energy & Entropy
Accuracy	77.3%	90.9%
False Alarm Rate	4.5%	0%
Missed Detection Rate	18.2%	9.1%

training each time. In this way, all of the target and ghost/clutter regions in the dataset were used for both training and testing. We used a value of K=3 for the K-NN classifier. Table 1 (second column) provides the corresponding values of the performance metrics. We note that the classification accuracy is 77.3%, with 4.5% false alarms and 18.2% missed detections.

Next, having identified the dominant features as energy and entropy, we proceed with classification using only the aforementioned textural features extracted from the 26 GLCMs. The new feature vector length is 52. The third column of Table 1 provides the corresponding values of the performance metrics when a K-NN classifier with cross-validation was used for K=3. We observe that, compared to the full feature set case, the classification accuracy has increased by 13.6% with no false alarms and a 9.1% reduction in missed detections. This validates the improved performance of the selected features in discriminating humans from ghosts/clutter.

5. CONCLUSION

In this paper, we presented decision tree analysis to identify the dominant and most discriminating GLCM based textural features for improved capability to distinguish between targets and ghosts/clutter in through-the-wall radar imaging applications. For the data analyzed, the energy and entropy attributes were determined to be the most relevant amongst the set of five commonly used GLCM features, which also included contrast, correlation, and homogeneity. The performance of the feature based scheme based on the dominant attributes was evaluated using a K-Nearest Neighbor classifier. It was shown that, compared to the scheme based on all five attributes, the dominant features yielded a higher classification accuracy, with lower number of false alarms and missed detections.

ACKNOWLEDGMENT

This work was supported by DRDC under Contract W7714-125544/00 l/SV.

REFERENCES

[1] Amin, M., [Through the Wall Radar Imaging], CRC Press, Boca Raton, (2010).
[2] Amin, M. G. and Ahmad, F., "Through-the-wall radar imaging: theory and applications," in R. Chellappa and S. Theodoridis (Eds.), [Academic Press Library in Signal Processing, Volume 2: Communications and Radar Signal Processing], Elsevier, (2013).
[3] Debes, C., Amin, M. G. and Zoubir, A. M., "Target detection in single- and multiple-view through-the-wall radar imaging," IEEE Trans. Geosci. Remote Sens. 47(5), 1349-1361 (2009).
[4] Mostafa, A.A and Zoubir, A.M., "3D target detection in through-the-wall radar imaging," Proc. SPIE 7697, 76971F (2010).
[5] Amin, M. G., Setlur, P., Ahmad, F., Sevigny, P. and DiFilippo, D., "Histogram based segmentation for stationary indoor target detection," Proc. SPIE 8361, 83610M (2012).
[6] Seng, C. H., Amin, M. G., Ahmad, F. and Bouzerdoum, A., "Image segmentations for through-the-wall radar target detection," IEEE Trans. Aerosp. Electronic Syst. 49(3), 1869-1896 (2013).
[7] Sengur, A., Amin, M., Ahmad, F., Sévigny, P., and DiFilippo, D., "Textural feature based target detection in through-the-wall radar imagery," Proc. SPIE 8714, 87140N (2013).

[8] Mostafa, A. A., [Segmentation and Classification for Through-the-Wall Radar Imaging], Ph.D. Thesis, TU Darmstadt, Germany, (2012).
[9] Harlick, R. M., Shanmugam, K. and Dinstein, I., "Textural features for image classification," IEEE Trans. Syst., Man, Cybern. Syst. SMC-3(6), 610-621 (1973).\
[10] Peckinpaugh, S., "An improved method for computing gray-level co-occurrence matrix based texture measures," Computer Vision, Graphics, and Image Proc.: Graphical Models and Image Proc. 53(6), 574–580 (1991).
[11] Chaddad, A., Tanougast, C., Dandache, A., Al Houseini, A., and Bouridane, A., "Improving of colon cancer cells detection based on Haralick's features on segmented histopathological images," Proc. IEEE Int. Conf. Computer Applications and Industrial Elect., 87-90 (2011).
[12] Breiman, L., Friedman, J., Olshen, R. and Stone, C., [Classification and Regression Trees], Wadsworth Int. Group, (1984).
[13] Fix, E. and Hodges, J., "Nonparametric Discrimination: small sample performance," in B. V. Dasarathy (Ed.), [Nearest Neighbor (NN) Norms: NN Pattern Classification Techniques], IEEE Computer Society Press, Los Alamitos, CA, (1991).
[14] Hart, P., "The Condensed Nearest Neighbour Rule," IEEE Trans. Inf. Theory. 14(3), 515-516 (1968).
[15] Sévigny, P., DiFilippo, D., Laneve, T., Chan, B., Fournier, J., Roy, S., Ricard, B. and Maheux, J., "Concept of operation and preliminary experimental results of the DRDC through-wall SAR system," Proc. SPIE 7669, 766907 (2010).
[16] Tsai, F., Chang, C.-K., Rau, J.-Y., Lin, T.-H. and Liu, G.-R.,"3D computation of gray level co-occurrence in hyperspectral image cubes," Lecture Notes in Computer Science 4679, 429-440 (2007).
[17] Gadkari, D., [Image quality analysis using GLCM], M.S. Thesis, University of Central Florida, Orlando, FL, (2004).
[18] Raut, S. and Petosa, A., "A compact printed bowtie antenna for ultra-wideband applications," Proc. European Microwave Conf., 81-84 (2009).
[19] Stone, M., "Cross-validatory choice and assessment of statistical predictions," J. Roy. Statist. Soc. Ser. B. 36, 111–147 (1974).
[20] Tan, P.-N., Steinbach, M. and Kumar, V., [Introduction to Data Mining], Addison-Wesley, (2006).